Chapter 2
Fire/Climate Interactions in Siberia

H. Balzter, K. Tansey, J. Kaduk, C. George, F. Gerard, M. Cuevas Gonzalez, A. Sukhinin, and E. Ponomarev

Abstract This paper presents an intercomparison of two burned area datasets, the L3JRC daily global burned area dataset derived from SPOT-VEGETATION and the FFID burned area dataset from MODIS. Burned area dynamics are presented and the influence of climate on the fire regime is discussed. Feedbacks of the fire dynamics to the climate system are evaluated. The Russian fire danger index is presented and compared to satellite observations of fires.

Keywords Climate • Fire • Temperature • Arctic oscillation • Remote sensing

2.1 The Fire Regime in Siberia

The circumpolar boreal forest covers approximately 1.37 billion hectares, or 9.2% of the world's land surface. Siberia is a hotspot for climate change. As a temperature controlled region it is particularly sensitive to even small increases in temperatures. In addition to this heightened vulnerability, the observed warming trend is more than twice as high as the global average, and climate model predictions show that this faster regional warming is likely to continue. Annual temperature anomalies

H. Balzter (✉), K. Tansey, and J. Kaduk
Department of Geography, Centre for Environmental Research, University of Leicester, University Road, Leicester LE1 7RH, UK
e-mail: hb91@le.ac.uk; kjt7@le.ac.uk; j.kaduk@leicester.ac.uk

C. George, F. Gerard, and M.C. Gonzalez
Centre for Ecology and Hydrology, Maclean Building, Benson Lane, Crowmarsh Gifford, Wallingford, Oxfordshire OX10 8BB, UK
e-mail: ctg@ceh.ac.uk; ffg@ceh.ac.uk; cuevasgonzalez@gmail.com

A. Sukhinin and E. Ponomarev
Siberian branch of Russian Academy of Sciences, VN Sukachev Institute of Forest, Academgorogok, Krasnoyarsk 660036, Russia
e-mail: boss@ksc.krasn.ru; evg@ksc.krasn.ru

H. Balzter (ed.), *Environmental Change in Siberia: Earth Observation, Field Studies and Modelling*, Advances in Global Change Research 40,
DOI 10.1007/978-90-481-8641-9_2,

since 1850 over central Siberia show a trend towards warmer temperatures at a higher rate than the global average, and with a faster increase after 1990 (Balzter et al. 2007).

The boreal forest is governed by fires, which generate a patchy mosaic of regenerating forest types. Lightning frequency, litter layer fuel mass and fuel moisture content all impact on the fire regime and are linked to meteorological conditions. Under scenarios of climate change many predictions show an acceleration of the fire regime. Many fires are also human-induced. Both climate and human population effects have been documented by Jupp et al. (2006). Greenhouse gas emissions from fires are an important component in the global carbon cycle. Fire is arguably the most important ecological disturbance worldwide releasing approximately 3.5 Pg C per year to the atmosphere (van der Werf et al. 2004). For the 1997/1998 carbon dioxide anomalies it is thought that 66% of the growth rate anomaly can be attributed to global biomass burning, of which 10% originated from the global boreal biome (van der Werf et al. 2004). It has been hypothesised that increasing greenhouse gas emissions from an accelerating fire regime could lead to a positive feedback with global warming (Amiro et al. 2001). Anticipated future climate change in the Northern Hemisphere with an increasingly dry and hot summer climate and an extended growing season could potentially lead to increased insect infestations and increased susceptibility of boreal trees to fire (Ayres and Lombardero 2000; Kobak et al. 1996).

Some authors have suggested that the fire regime in the boreal biome is coupled to the climate system through large-scale atmospheric circulation patterns, e.g. (Balzter et al. 2005, 2007; Hallett et al. 2003). Atmospheric oscillation patterns have an impact on regional climatic variability and consequently vegetation activity. Los et al. (2001) and Buermann et al. (2003) found that two predominant hemispheric-scale modes of covariability are related to teleconnections associated with the El Niño Southern Oscillation (ENSO) and the Arctic Oscillation (AO): The warm event ENSO signal is associated with warmer and greener conditions in far East Asia, while the positive phase of the AO leads to enhanced warm and green conditions over large regions in Asian Russia.

In the recent past Siberia has experienced extreme fire years (Sukhinin et al. 2004), which coincided with years in which the AO was in a more positive phase (Balzter et al. 2005). Jupp et al. (2006) found that regional clusters of fire scars in Siberia occurred in places with dry precipitation anomalies at scales of tens of kilometers. An analysis of surface air temperature and precipitation at ten meteorological stations in West Siberia by Frey and Smith (2003) showed that West Siberia shows increases in temperature and precipitation, particularly springtime warming and more winter precipitation. Frey and Smith (2003) found an association of autumn and winter temperatures with the AO. On average, the AO was linearly correlated with 96% (winter), 19% (spring), 0% (summer), 67% (autumn), and 53% (annual) of the warming (Frey and Smith 2003).

The AO has shown a statistically significant trend towards the positive phase between 1950 and the present day (Balzter et al. 2007), which is likely to indicate

global climate change trends. Overland et al. (2002) observed a shift in wind fields from anomalous north-easterly flows in the 1980s to anomalous south-westerly flows in the 1990s during March and April in Siberia, coinciding with a systematic shift in the AO near the end of the 1980s. These hemispheric-scale changes in the heat transport from the oceans to continental parts of Siberia could have major repercussions for the fire regime (Balzter et al. 2005, 2007). The AO is also influenced by intense volcanic eruptions, which inject aerosols into the stratosphere and via an enhanced temperature gradient between the pole and the tropics lead to an acceleration of the polar vortex (Stenchikov et al. 2006). This acceleration expresses itself as a positive phase of the AO.

The following sections describe two remotely sensed burned area datasets, followed by a discussion of the impacts of climate on fire, and the feedbacks of fire on the climate system.

2.2 The L3JRC Global Daily Burned Area Dataset

Due to the extent and remoteness of Siberia the only cost effective way of monitoring the fire regime is using remote sensing. A global daily burned area dataset at 1 km spatial resolution is available from the VEGETATION sensor aboard the SPOT satellite. A single algorithm was used to classify burnt areas from the spectral reflectance data. SPOT 4 was launched in 1998 into a polar sun synchronous orbit at 832 km. The algorithm is described in Tansey et al. (2008), and is based primarily on the 0.83 μm near-infrared (NIR) channel.

Burned forest area statistics were extracted by overlaying administrative regions as vectors, reprojecting the L3JRC datasets to the Albers equal area projection and calculating polygon statistics in the programming language R. Forest areas were defined using the Global Land Cover 2000 map (Bartalev et al. 2003) as any of the land cover classes "Evergreen Needle-leaf Forest" (class 1), "Deciduous Broadleaf Forest" (3), "Needle-leaf/Broadleaf Forest" (4), "Mixed Forest" (5), "Broadleaf/Needle-leaf Forest" (6), "Deciduous Needle-leaf Forest" (7), "Broadleaf deciduous shrubs" (8), "Needle-leaf evergreen shrubs" (9), "Forest-Natural Vegetation complexes" (21) or "Forest-Cropland complexes" (22). On the assumption that the fire season is constrained by the winter time to be between Julian dates 161 and 272, any burned areas that were detected outside this date range were masked out. This matches the date range used in generating the FFID burned area dataset (next section). Table 2.1 gives the L3JRC burned forest area for each administrative region (oblast) obtained in this way. It shows that some oblasts have a stable fire regime but in others a large interannual variability is observed. The standard deviation between years as a measure of interannual variability reveals that Yakutia Republic, Evenk a.okr., Irkutsk oblast, Chita oblast, Buryat Republic, Khabarovsk Kray, Amur oblast, Magadan oblast, Chukchi a.okr., Krasnoyarsk Kray

Table 2.1 Annual burned area statistics (km²) per oblast (administrative region) based on the L3JRC global daily burned area dataset. Only forest areas (based on GLC2000) and Julian dates 161–272 were analysed

OBLAST	2000	2001	2002	2003	2004	2005	2006
Adigei Republic	27	54	6	27	8	25	51
Aga-Buryat a.okr.	64	19	3	327	121	15	54
Altai Kray	115	92	124	88	82	142	164
Amur oblast	2,493	869	2,632	3,708	1,841	1,333	5,048
Arkhangelsk oblast	4	4	9	2	5	9	3
Astrakhan oblast	0	0	0	1	3	0	9
Bashkortostan Republic	288	304	154	166	97	444	549
Belgorod oblast	112	58	65	47	47	57	181
Bryansk oblast	8	0	29	0	0	9	5
Buryat Republic	4404	1,656	1,235	7,695	2,771	2,964	4,918
Checheno-Ingush Republic	0	0	0	0	0	0	0
Chelyabinsk oblast	22	111	23	82	85	108	63
Chita oblast	5,625	2,128	1,176	9,505	4,590	4,212	6,493
Chukchi a.okr.	995	986	1,587	3,025	1,829	488	2,752
Chuvash Republic	21	74	31	2	3	12	12
Daghestn Republic	0	0	0	0	0	0	4
Evenk a.okr	1,026	713	804	10,895	2,960	8,002	10,582
Gorno-Altai Republic	202	78	649	548	490	539	409
Irkutsk oblast	2,916	1,464	1,715	4,868	1,461	7,127	9,744
Ivanovo oblast	0	1	20	0	0	0	0
Kabardino-Balkarian Republic	3	0	0	0	1	0	0
Kaliningrad oblast	0	0	13	2	0	0	1
Kalmyk-Khalm-Tangch Republic	2	2	1	4	2	1	1
Kaluga oblast	0	1	29	0	0	0	0
Kamchatka oblast	686	50	153	153	398	245	77
Karachai-Cherkess Republic	4	6	2	2	0	2	3
Karelia Republic	6	3	0	4	0	4	4
Kemerovo oblast	5	20	196	59	39	23	99
Khabarovsk Kray	6,469	2,344	4,232	6,130	4,482	6,171	4,740
Khakass Republic	12	15	38	49	27	73	60
Khanty-Mansi a.okr.	166	79	82	200	216	167	303
Kirov oblast	9	3	0	0	1	9	4
Komi Republic	216	214	211	33	96	73	60
Koryak a.okr.	940	761	311	1,085	343	331	529
Kostroma oblast	0	4	5	0	0	1	0
Krasnodar Kray	563	846	312	642	469	537	986
Krasnoyarsk Kray	999	660	539	2,495	1,988	949	1,528
Kurgan oblast	104	149	46	225	164	90	130
Kursk oblast	96	35	37	10	23	42	46
Leningrad oblast	0	0	4	0	2	0	24
Lipetsk oblast	95	159	93	54	146	235	135

(continued)

Table 2.1 (continued)

OBLAST	2000	2001	2002	2003	2004	2005	2006
Magadan oblast	5,186	3,329	3,265	6,878	3,574	3,097	4,499
Mari-El Republic	0	1	1	0	0	0	0
Mordovian SSR	30	50	49	2	12	24	8
Moscow oblast	1	9	47	0	0	6	2
Murmansk oblast	7	59	65	164	93	58	22
Nenets a.okr.	9	13	38	13	17	14	20
Nizhni Novgorod oblast	14	47	110	15	8	34	13
North-Ossetian SSR	0	0	0	0	0	0	0
Novgorod oblast	0	0	0	1	0	0	0
Novosibirsk oblast	59	74	31	109	91	105	229
Omsk oblast	22	174	66	21	16	18	23
Orenburg oblast	63	133	116	79	98	219	185
Oryel oblast	91	108	44	15	36	79	15
Penza oblast	168	173	108	32	75	93	44
Perm oblast	12	69	10	22	10	50	14
Primorski Kray	1	16	6	253	41	50	57
Pskov oblast	0	0	19	1	0	0	1
Rostov oblast	215	319	315	220	394	296	324
Ryazan oblast	137	96	238	19	92	112	56
Sakhalin oblast	66	14	8	208	23	39	12
Samara oblast	159	328	309	149	123	319	184
Saratov oblast	208	318	184	198	313	429	312
Smolensk oblast	0	0	22	0	0	0	0
Stavropol Kray	86	212	66	123	119	155	315
Sverdlovsk oblast	19	55	76	143	86	374	28
Tambov oblast	181	316	241	113	238	348	251
Tatarstan Republic	484	431	554	172	158	282	201
Taymyr a.okr.	45	37	1	287	164	193	187
Tomsk oblast	42	152	395	110	689	66	225
Tula oblast	59	188	206	14	20	97	30
Tuva Republic	1,055	812	2,464	1,557	757	827	1,667
Tver oblast	2	2	47	0	0	1	1
Tyumen oblast	71	260	128	298	146	150	129
Udmurt Republic	3	2	0	0	21	2	0
Ulyanovsk oblast	243	291	146	73	56	173	117
Ust-Orda Buryat a.okr.	67	38	29	254	42	131	87
Vladimir oblast	0	2	21	0	5	0	0
Volgograd oblast	38	79	72	64	72	60	78
Vologda oblast	1	10	7	2	0	2	0
Voronezh oblast	287	334	214	187	272	214	274
Yakutia Republic	18,684	19,623	38,307	44,691	29,326	73,500	56,497
Yamalo-Nenets a.okr.	474	263	95	497	713	386	500
Yaroslavl oblast	1	2	22	1	0	0	0
Yevrey a.oblast	14	9	4	62	6	15	198
Russia	57,001	42,410	64,712	109,180	62,696	116,457	116,576

and Tuva Republic (in descending order) show the highest variability between years, with standard deviations exceeding 500 km^2 year^{-1}. Yakutia, the largest oblast covering more than 3,100,000 km^2 of the ~17,000,000 km^2 of Russia, also shows the highest mean burned forest area over the observed years.

2.3 Forest Fire Intensity Dynamics (FFID) Daily Burn Scar Identification

Using moderate resolution sensors (approx. 1 km^2 pixels 2,000 km swath width) that have a repeat time of 1 day or less in boreal regions, it is possible to determine the date when a fire occurred during cloud-free conditions. This method was investigated in the FFID project (Forest Fire Intensity Dynamics). For the FFID Daily Burned Area product, instead of using thermal sensors for detecting active fires which can then be missed due to cloud or smoke for example, a vegetation index differencing approach is used which is able to discriminate disturbances long after the event has occurred. The parameter used was the Normalised Difference Short-Wave Infrared Index (NDSWIR), a combination of the near-infrared (NIR) and short-wave infra-red (SWIR) signals, which is sensitive to vegetation water content, and so can be used as a proxy for canopy density (George et al. 2006).

$$NDSWIR = \frac{(\rho 858\,\text{nm} - \rho 1640\,\text{nm})}{(\rho 858\,\text{nm} + \rho 1640\,\text{nm})} \tag{2.1}$$

The satellite data used was the Terra-MODIS Nadir BRDF-Adjusted Reflectance (NBAR) 16-Day composite (MOD43B4) (Friedl et al. 2002), which has reduced view angle effects that are present in wide view-angle sensors. The NBAR data provide a nadir adjusted value of reflectance in each of seven bands once in every 16-day period. The removal of view angle effects and the adjustment to the mean solar zenith angle (of the 16-day period) produce a stable, consistent product allowing the spatial and temporal progression of phenological characteristics to be easily detected (Schaaf et al. 2002). A MODIS data granule is 1,200 × 1,200 pixels, each pixel being 927.4 m on a side.

At the northern reach of the boreal zone (approx. 70°N) the growing season is very short so only the composites from mid July to mid September were included to reduce any phenological effects. To keep the methodology consistent the same period was used at the lower latitudes even though these areas had a much longer growing season. The four composites within this time period were used to produce the NDSWIR layers. For each of the four NDSWIR layers within a year, a NDSWIR difference layer was calculated by subtracting that layer from the corresponding layer from the previous year. This difference layer would then show a high value where there was a large decrease in biomass, and a low value for those areas of little change. The four difference images for each year were then combined to give

one annual difference image (ADI). This annual difference greyscale image, ranged from low values of no change to higher values showing missing biomass compared with the previous year. To set the threshold to separate out burned areas, MODIS thermal anomalies (TA) (Justice et al. 2002), which give the location and Julian Day of active fires, were used. This assumed that if a TA were present, then that ADI pixel had burned. Then for each of the IGBP woody land covers (classes 1–8) within a granule, the mean ADI value under the TA's were calculated, and this value was used to set the threshold for that land cover class. The result is a binary mask, with 1's representing disturbance scars. However, this layer will also show other disturbances apart from burning, such as insect infestations, wind blow or logging. It also doesn't show the date of burning. To identify and date any burns, the TA's are used again. Any scars not overlain with TA's are discarded. For the remaining scars, the pixels corresponding to the TA's are assigned the Julian Day of that TA. This leaves many of the burned areas being a combination of dated pixels and undated pixels, the undated pixels being where perhaps there was too much cloud or smoke for an active fire to be detected, but where there was still a significant reduction in vegetation biomass. These undated pixels are then dated by extrapolating from the dated pixels. The result is a raster with each burnt pixel having a value of the Julian Day when it was burnt.

Table 2.2 shows the FFID burned area for each administrative region (oblast).

Table 2.2 Annual burned forest area statistics (km^2) per oblast (administrative region) based on the FFID dataset

OBLAST	2001	2002	2003	2004	2005	2006
Adigei Republic	0	0	0	0	0	0
Aga-Buryat a.okr.	473	58	3,452	298	243	205
Altai Kray	7,637	8,594	9,485	6,087	5,289	5,049
Amur oblast	13,278	20,096	33,445	5,972	9,817	20,172
Arkhangelsk oblast	530	274	173	292	189	317
Astrakhan oblast	0	0	0	0	0	0
Bashkortostan Republic	2,126	1,217	1,424	1,816	510	2,087
Belgorod oblast	1,189	1,124	96	120	373	408
Bryansk oblast	422	1,780	256	259	463	1,388
Buryat Republic	1,035	1,617	43,649	1,165	2,616	2,457
Checheno-Ingush Republic	0	0	0	0	0	0
Chelyabinsk oblast	4,628	1,806	2,080	3,062	845	2,197
Chita oblast	4,947	5,436	78,097	5,226	5,031	11,432
Chukchi a.okr.	2,177	3,295	10,944	500	587	106
Chuvash Republic	142	75	24	80	148	342
Daghestn Republic	0	0	0	0	0	0
Evenk a.okr	80	623	167	102	964	6,731
Gorno-Altai Republic	275	190	309	129	16	30
Irkutsk oblast	3,837	6,756	26,583	2,578	3,080	13,194
Ivanovo oblast	40	559	32	28	60	681

(continued)

Table 2.2 (continued)

OBLAST	2001	2002	2003	2004	2005	2006
Kabardino-Balkarian Republic	0	0	0	0	0	0
Kaliningrad oblast	88	299	329	281	192	561
Kalmyk-Khalm-Tangch Republic	0	0	0	0	0	0
Kaluga oblast	30	1,392	156	103	109	1,549
Kamchatka oblast	1,730	574	556	83	117	181
Karachai-Cherkess Republic	0	0	0	0	0	0
Karelia Republic	66	82	181	28	144	234
Kemerovo oblast	1,192	3,906	2,394	3,306	2,365	1,296
Khabarovsk Kray	6,423	7,375	16,696	3,020	11,260	4,086
Khakass Republic	588	1,671	594	992	1,225	390
Khanty-Mansi a.okr.	691	597	1,914	7,569	5,434	3,703
Kirov oblast	522	344	218	172	241	743
Komi Republic	941	68	57	242	127	97
Koryak a.okr.	1,294	1,276	3,759	200	287	390
Kostroma oblast	178	258	39	32	68	482
Krasnodar Kray	0	0	0	0	0	0
Krasnoyarsk Kray	3,925	6,859	10,013	7,868	7,336	11,214
Kurgan oblast	1,002	774	1,383	5,046	421	2,212
Kursk oblast	1,895	2,895	243	1,206	2,089	1,071
Leningrad oblast	68	1,397	183	277	303	2,143
Lipetsk oblast	1,866	2,002	378	1,361	2,106	1,018
Magadan oblast	6,248	1,993	9,871	762	365	564
Mari-El Republic	78	167	21	55	67	226
Mordovian SSR	681	729	187	464	528	1,283
Moscow oblast	83	2,339	237	208	101	1,755
Murmansk oblast	162	127	174	121	130	67
Nenets a.okr.	7	0	5	38	6	26
Nizhni Novgorod oblast	796	1,113	152	394	659	1,711
North-Ossetian SSR	0	0	0	0	0	0
Novgorod oblast	94	710	106	269	40	1,107
Novosibirsk oblast	9,184	8,082	6,641	9,180	7,415	16,584
Omsk oblast	5,436	3,237	2,568	7,551	1,777	6,784
Orenburg oblast	5,112	4,398	4,968	4,815	5,165	3,931
Oryel oblast	1,417	2,337	142	1,303	1,225	1,335
Penza oblast	1,701	1,434	532	1,023	1,052	2,812
Perm oblast	439	98	83	99	135	482
Primorski Kray	4,275	1,675	4,759	4,069	2,191	2,874
Pskov oblast	283	2,010	251	668	222	2,922
Rostov oblast	17	13	1	1	11	3
Ryazan oblast	775	1,929	261	876	1,188	2,142
Sakhalin oblast	208	540	1,169	102	68	100

(continued)

Table 2.2 (continued)

OBLAST	2001	2002	2003	2004	2005	2006
Samara oblast	2,105	3,432	1,187	1,735	1,549	2,161
Saratov oblast	3,402	4,459	1,976	3,439	5,775	3,696
Smolensk oblast	206	3,652	966	559	58	3,916
Stavropol Kray	0	0	0	0	0	0
Sverdlovsk oblast	558	796	673	2,938	716	3,275
Tambov oblast	3,147	3,082	1,005	1,687	2,402	2,156
Tatarstan Republic	1,694	1,733	962	1,480	706	1,435
Taymyr a.okr.	68	29	28	43	39	176
Tomsk oblast	1,144	1,177	4,413	5,117	4,307	4,192
Tula oblast	791	1,515	163	851	1,005	1,814
Tuva Republic	1,184	8,383	1,771	221	736	532
Tver oblast	74	2,515	667	187	117	1,736
Tyumen oblast	1,194	638	2,288	7,676	741	5,560
Udmurt Republic	124	108	90	38	65	265
Ulyanovsk oblast	838	1,192	590	996	930	1,818
Ust-Orda Buryat a.okr.	186	708	3,010	39	482	836
Vladimir oblast	144	1,232	49	106	58	529
Volgograd oblast	2,713	2,403	905	1,553	2,822	1,398
Vologda oblast	173	581	99	54	116	532
Voronezh oblast	2,972	3,131	780	1,526	2,275	1,248
Yakutia Republic	36,534	58,789	22,535	1,875	11,259	3,793
Yamalo-Nenets a.okr.	539	1,015	774	1,145	3,717	3,067
Yaroslavl oblast	68	735	201	35	60	1,102
Yevrey a.oblast	2,769	1,945	3,193	3,847	3,510	1,878
Russia	164,940	221,451	329,761	128,643	129,841	191,992

2.4 Burned Forest Area Intercomparison

An intercomparison of the L3JRC and FFID datasets with other published burned area data by Soja et al. (2004) and George et al. (2006) was carried out, the results of which are shown in Fig. 2.1. The study region "SIBERIA-2" is the same as in George et al. (2006) since this was the largest common area coverage. The SIBERIA-2 region covers over 3 million km^2 of Central Siberia, and includes Irkutsk Oblast, Krasnoyarsk Kray, Taimyr, Khakass Republic, Buryat Republic and Evenksky Autonomous Oblast (approximately 79–119°E, 51–78°N). Figure 2.1 shows several catastrophic fire years in the Central Siberian region: 1992–1993, 2003 and 2006 showed large forest fires. When comparing the different datasets it becomes apparent that while in most cases the interannual variability is similar, but in particular years there are large uncertainties in the estimates.

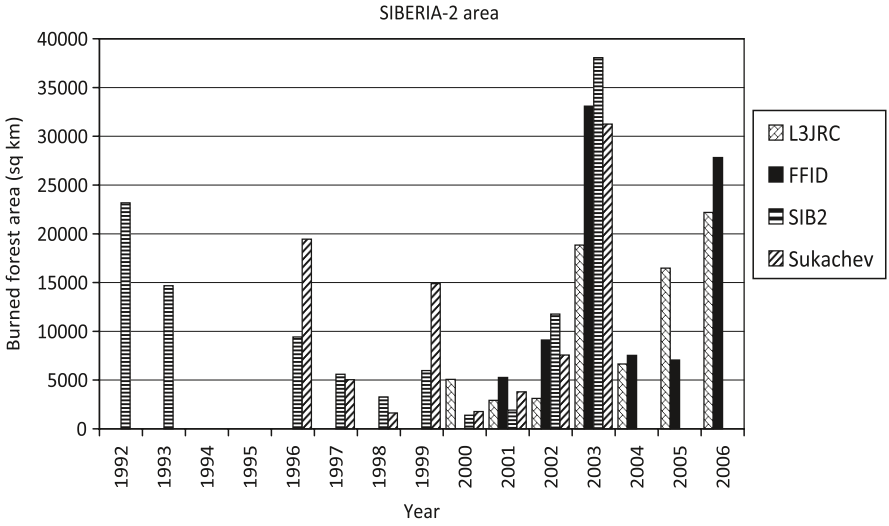

Fig. 2.1 Intercomparison of annual burned forest area estimates from the datasets L3JRC, FFID, L3JRC, SIBERIA-2, and SUKACHEV. The datasets cover different time ranges, only 2001–2003 is the common temporal coverage

2.5 Climate Impacts on Fire

Observations from remote sensing have shown that large-scale climate oscillations, in particular the Arctic Oscillation, are thought to have an impact on forest fire frequency in Central Siberia (Balzter et al. 2005, 2007). Climate data have shown and climate models predict that the Arctic Oscillation responds to large-scale volcanic eruptions such as the Mount Pinatubo eruption in 1991, which injected large amounts of aerosols into the lower stratosphere and changed global climate for several years (Stenchikov et al. 2002, 2006). Volcanic eruptions can lead to a positive phase of the Arctic Oscillation (Stenchikov et al. 2002, 2006), which in turn provides conditions that are conducive to extreme forest fires (Balzter et al. 2005).

Central Siberia contains several climatic and ecological zones. As a result many authors have noted specific fire regimes influencing different forest types in the region. The fire regime influences the duration of the fire season and the spatial patterns of forest fires locations (Ivanova et al. 2005, Kurbatski and Ivanova 1987, Valendick and Ivanova 2001). The degree of forest fine fuel to be ignited is determined by the variation of fuel moisture content, which is dependent on the length of the dry period. Forest fire initiation and fire spread across the ground cover is possible if the moisture content of fine fuels reaches a fixed low value after which this parameter changes only slightly. In particular, for the needles of conifers (except larch) the balanced moisture content is 11–26% depending on relative

humidity, and for leaves of deciduous trees, needles of larch and grasses it is 9–31% (Kurbatski et al. 1987).

Mass forest fire ignitions are caused mostly under the influence of atmospheric anticyclones. The moisture content of fine fuels decreases to 9–30% and an extreme fire danger state evolves after 85–150 h under these conditions without precipitation. An uncontrollable situation develops if forest fires cannot be localized and extinguished at an early stage.

Experimental data of the last 10 years show the interconnection between local fire activity and local weather conditions forming at the same point in time. This interconnection is determined by a formation of stable anticyclones with lifetimes up 30–90 days over the region. Usually the process can be observed over regions where mass forest fires burned at the same time. The exact physical processes have not yet been described. However, it can be hypothesised that stable anticyclone weather formations are influenced by convective heat flow from the epicentre of active forest fires. This formed high-pressure zone ejects other cyclones and cumulonimbus clouds.

The forest fire danger condition is characterized by the Russian fire danger index (FD) that can be calculated using daily air temperature and dew point temperature measurements during the fire season. This index forecasts the degree of forest fine fuel dryness and fire ignition ability indirectly. At the same time the value of this index and the persistence of high values of the fire danger characterize not only the forest fire danger state but also weather condition features formed by fire convection flow.

According to experimental data, certain values of the FD index were identified by Russian researchers for different stages of forest fire danger. An extreme fire danger level in the forests of Central Siberia is present when FD reaches values of 3,000–4,200. However, during last 10 years this index has been observed to be much higher after long droughts. For example, the rain-free period in the Angara river forests in 2006 was over 50 days (Fig. 2.2). In Yakutia in the middle of the summer anticyclone periods are dominating over 60 days annually. During these times the fire danger index can be between 14,000 and 20,000. As Fig. 2.2 shows, the Russian fire danger index is correlated with the Duff Moisture Code (DMC) of the Canadian Forest Fire Weather System, although a slight temporal phase is noticeable.

Consequences of long droughts affect fire locating and extinguishing statistics. Wildfires should be detected at the early stage of burning to enable efficient and effective fire prevention measures. However, in a case of an extreme fire situation non-localized fires are uncontrollable when fire fighting cannot extinguish them efficiently anymore. Under these conditions forest fires can be active for about 30 days. In 2007 the percentage of fires that was located during the first day of activity was about 88% (see Fig. 2.3).

Figure 2.3 is illustrating the opportunity of forest fire prevention measures according to material and technical support level. The annual part of large fires (area more than 1,000 ha) that amount to not more than 5% of the total fire statistics but up to 90% of the total damaged forest area – provides an objective appraisal for the region.

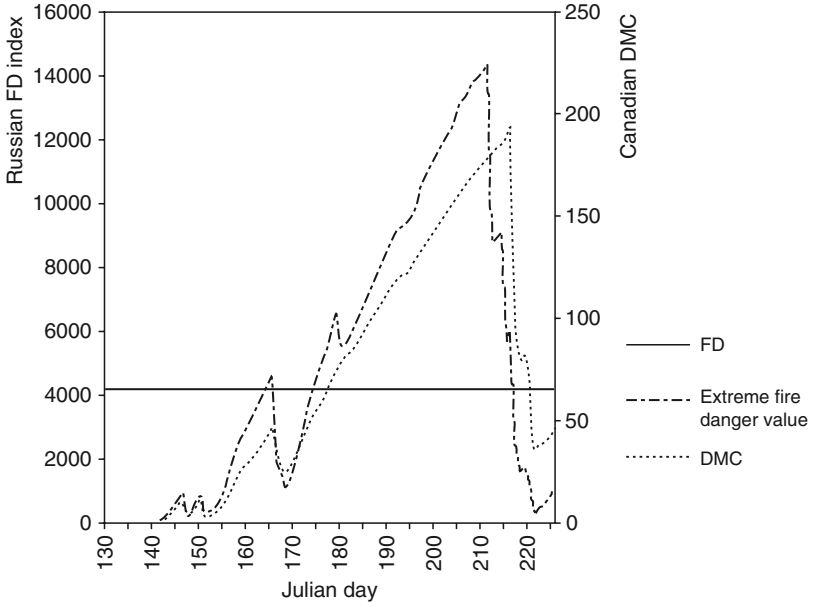

Fig. 2.2 Extreme fire danger index dynamics in the Angara River region, from data recorded at Kezhma meteostation for the fire danger season of 2006. The Canadian Duff Moisture Code (DMC) is shown for comparison

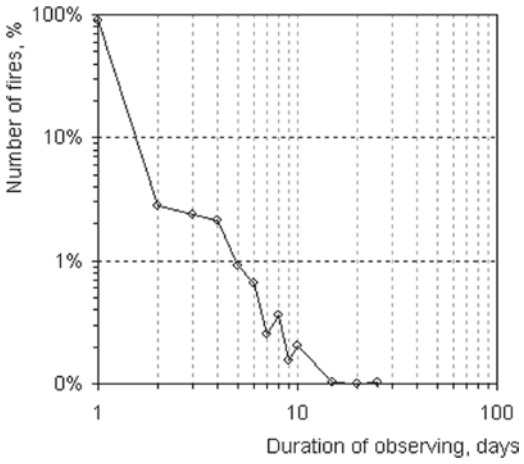

Fig. 2.3 Frequency distribution of the duration of active forest fires in the Krasnoyarsk region, 2007. About 97% of the fires burned only for 1–2 days, and only 1% of fires burned for longer than 5 days

The FD index is effective at detecting conditions that enhance extreme fire activity. The number of days on which the FD index exceeds 4,200 explains about half the interannual variability in burned area in the Krasnoyarsk administrative region determined from the FFID remotely sensed dataset (Fig. 2.4).

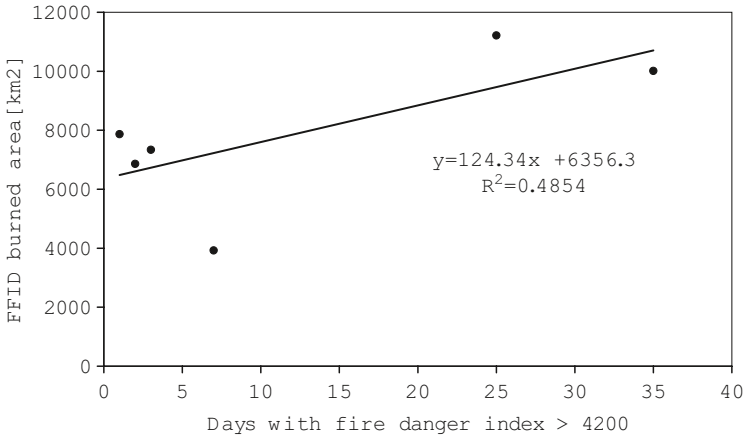

Fig. 2.4 Regression analysis of remotely sensed burned area from the FFID project (km^2) and the number of days with a fire danger index exceeding 4,200 for the Krasnoyarsk region. *Data points* represent the years 2001–2006

Thus, weather conditions are determining the characteristics of the fire season in Siberia. The frequency of prolonged droughts has been observed to increase. Mass forest fire activity is influenced by extreme weather conditions forming at a regional level.

2.6 Fire Feedbacks to the Climate System

Depending on the dominant processes, biosphere feedbacks to the climate system can accelerate or slow down climate change (Cox et al. 2000). Fluxes of heat, water, carbon, and other greenhouse gases between the land surface and the atmosphere interact in complex nonlinear ways (Delworth and Manabe 1993). Siberian forest fires feed back to the climate system by (i) emitting trace gases that contribute to the greenhouse effect, (ii) emitting aerosols that reflect incoming solar radiation back to space having a net cooling effect, (iii) disrupting carbon sequestration by destroying vegetation that would otherwise take up carbon dioxide through photosynthesis, (iv) changing the heterotrophic respiration in the soil, (v) depositing char and charcoal particles and dust on the ground that can be subject to infiltration into the soil or erosion after rainfall and sedimentation downstream, (vi) changing the water balance because of vegetation destruction leading to dryer conditions and increased repeat fire risk in the fire scar, (vii) changing the albedo (proportion of reflected incoming radiation).

Quantitative trace gas emission estimates from forest fires in Siberia are still subject to considerable uncertainty. Soja et al. (2004) estimate that from 1998 to 2002 direct carbon emissions during forest fires quantified by a mean standard

emission scenario amount to 555–1031 Tg CO_2, 43–80 Tg CO, 2.4–4.5 Tg CH_4 and 4.6–8.6 Tg carbonaceous aerosols. These emissions represent between 10% and 26% of the global emissions from forest and grassland fires (Soja et al. 2004).

A study of post-fire photosynthetic activity using MODIS fraction of absorbed photosynthetically active radiation (fAPAR) data over Siberian burn scars found that in the years immediately following a fire, fAPAR was reduced between 3% and 27% compared to unburned control plots (Cuevas-González et al. 2008). The amount of photosynthetic reduction depended on forest type and an interaction term of forest type/latitude of the site.

Randerson et al. (2006) studied one particular boreal forest fire in Alaska and quantified the effects of greenhouse gas emissions, aerosols, black carbon deposition on snow and sea ice, and post-fire changes in surface albedo on climate. The net radiative forcing effect was a net warming of 34 Wm^{-2} of burned area during the first year, but a net cooling effect of −2.3 Wm^{-2} over an 80 year period. The reason for this is that long-term increases in surface albedo can have a larger radiative forcing impact than greenhouse gas emissions from the fire (Randerson et al. 2006). However, whether these results are applicable to the entire boreal biome is questionable.

2.7 Conclusions

Siberian forest fires are significant as a factor in the global carbon cycle because of their large interannual variability. Climate impacts on the frequency and extent of forest fires, and fires in turn feed back to the climate system via the atmosphere. Current scenarios of global change indicate that we are likely to see changes in the vegetation patterns and fire regime in Siberia. Satellite remote sensing has an important role to play in monitoring the evolving fire regime from space.

Acknowledgments The Global Land Cover 2000 database was generated by the European Commission, Joint Research Centre, 2003, http://www-gem.jrc.it/glc2000.

References

Amiro BD, Stocks BJ, Alexander ME, Flannigan MD, Wotton BM (2001) Fire, climate change, carbon and fuel management in the Canadian boreal forest. Int J Wildland Fire 10:405–413

Ayres MP, Lombardero MJ (2000) Assessing the consequences of global change for forest disturbance from herbivores and pathogens. Sci Total Environ 262:263–286

Balzter H, Gerard F, George C, Weedon G, Grey W, Combal B, Bartholome E, Bartalev S, Los S (2007) Coupling of vegetation growing season anomalies and fire activity with hemispheric and regional-scale climate patterns in central and east Siberia. J Climate 20:3713–3729

Balzter H, Gerard FF, George CT, Rowland CS, Jupp TE, McCallum I, Shvidenko A, Nilsson S, Sukhinin A, Onuchin A, Schmullius C (2005) Impact of the Arctic Oscillation pattern on interannual forest fire variability in Central Siberia. Geophys Res Lett 32:L14709

Bartalev SA, Belward AS, Erchov DV, Isaev AS (2003) A new SPOT4-VEGETATION derived land cover map of Northern Eurasia. Int J Remote Sens 24:1977–1982

Buermann W, Anderson B, Tucker CJ, Dickinson RE, Lucht W, Potter CS, Myneni RB (2003) Interannual covariability in northern hemisphere air temperatures and greenness associated with El Nino-Southern Oscillation and the Arctic Oscillation. J Geophys Res-Atmos 108:4396

Cox PM, Betts RA, Jones CD, Spall SA, Totterdell IJ (2000) Acceleration of global warming due to carbon-cycle feedbacks in a coupled climate model. Nature 408:184–187

Cuevas-González M, Gerard F, Balzter H, Riaño D (2008) Studying the change in fAPAR after forest fires in Siberia using MODIS, Int J Remote Sens, 29:23: 6873–6892. DOI: 10.1080/01431160802238427

Delworth T, Manabe S (1993) Climate variability and land-surface processes. Adv Water Resour 16:3–20

Frey KE, Smith LC (2003) Recent temperature and precipitation increases in West Siberia and their association with the Arctic Oscillation. Polar Res 22:287–300

Friedl MA, McIver DK, Hodges JCF, Zhang XY, Muchoney D, Strahler AH, Woodcock CE, Gopal S, Schneider A, Cooper A, Baccini A, Gao F, Schaaf C (2002) Global land cover mapping from MODIS: algorithms and early results. Remote Sens Environ 83:287–302

George C, Rowland C, Gerard F, Balzter H (2006) Retrospective mapping of burnt areas in Central Siberia using a modification of the normalised difference water index. Remote Sens Environ 104:346–359

Hallett DJ, Lepofsky DS, Mathewes RW, Lertzman KP (2003) 11000 years of fire history and climate in the mountain hemlock rain forests of southwestern British Columbia based on sedimentary charcoal. Can J Forest Res 33:292–312

Ivanova GA, Volosatova NA, Kukavskaya EA, McCrae DD, Conard SG (2005) Fire emission of carbon in pines of Central Siberia. Remote sensing in forestry. Devises and techniques. Institute for Forest, Krasnoyarsk, pp 51–54

Jupp TE, Taylor CM, Balzter H, George CT (2006) A statistical model linking Siberian forest fire scars with early summer rainfall anomalies. Geophys Res Lett 33:L14701

Justice CO, Giglio L, Korontzi S, Owens J, Morisette JT, Roy D, Descloitres J, Alleaume S, Petitcolin F, Kaufman Y (2002) The MODIS fire products. Remote Sens Environ 83:244–262

Kobak KI, Turchinovich IY, Kondrasheva NY, Schulze ED, Schulze W, Koch H, Vygodskaya NN (1996) Vulnerability and adaptation of the larch forest in eastern Siberia to climate change. Water Air Soil Pollut 92:119–127

Kurbatski NP, Ivanova GA (1987) Fire danger of pine forests of forest-steppe and its decreasing technique. Institute for Forest, Krasnoyarsk, 112 p

Los SO, Collatz GJ, Bounoua L, Sellers PJ, Tucker CJ (2001) Global interannual variations in sea surface temperature and land surface vegetation, air temperature, and precipitation. J Climate 14:1535–1549

Overland JE, Wang MY, Bond NA (2002) Recent temperature changes in the Western Arctic during spring. J Climate 15:1702–1716

Randerson JT, Liu H, Flanner MG, Chambers SD, Jin Y, Hess PG, Pfister G, Mack MC, Treseder KK, Welp LR, Chapin FS, Harden JW, Goulden ML, Lyons E, Neff JC, Schuur EAG, Zender CS (2006) The impact of boreal forest fire on climate warming. Science 314:1130–1132

Schaaf CB, Gao F, Strahler AH, Lucht W, Li X, Tsang T, Strugnell NC, Zhang X, Jin Y, Muller J, Lewis PE, Barnsley M, Hobson P, Disney M, Roberts G, Dunderdale M, Doll C, d'Entremont RP, Hug B, Liang S, Privette JL, Roy D (2002) First operational BRDF, albedo nadir reflectance products from MODIS. Remote Sens Environ 83:135–148

Soja AJ, Cofer WR, Shugart HH, Sukhinin AI, Stackhouse PW, McRae DJ, Conard SG (2004) Estimating fire emissions and disparities in boreal Siberia (1998–2002). J Geophys Res-Atmos 109:D14S06

Stenchikov G, Robock A, Ramaswamy V, Schwarzkopf MD, Hamilton K, Ramachandran S (2002) Arctic Oscillation response to the 1991 Mount Pinatubo eruption: Effects of volcanic aerosols and ozone depletion. J Geophys Res-Atmos 107:4803

Stenchikov G, Hamilton K, Stouffer RJ, Robock A, Ramaswamy V, Santer B, Graf HF (2006) Arctic Oscillation response to volcanic eruptions in the IPCC AR4 climate models. J Geophys Res-Atmos 111:D18101

Sukhinin AI, French NHF, Kasischke ES, Hewson JH, Soja AJ, Csiszar IA, Hyer EJ, Loboda T, Conrad SG, Romasko VI, Pavlichenko EA, Miskiv SI, Slinkina OA (2004) AVHRR-based mapping of fires in Russia: new products for fire management and carbon cycle studies. Remote Sens Environ 93:546–564

Tansey K, Grégoire J-M, Defourny P, Leigh R, Pekel J-F, van Bogaert E, Bartholomé E (2008) A new, global, multi-annual (2000–2007) burnt area product at 1 km resolution. Geophys Res Lett 35:L01401. doi:10.1029/2007GL031567

Valendick EN, Ivanova GA (2001) Fire regimes in forests of Siberia and Far East. Lesovedenie 4:69–76

van der Werf GR, Randerson JT, Collatz GJ, Giglio L, Kasibhatla PS, Arellano AF, Olsen SC, Kasischke ES (2004) Continental-scale partitioning of fire emissions during the 1997 to 2001 El Nino/La Nina period. Science 303:73–76

http://www.springer.com/978-90-481-8640-2

Environmental Change in Siberia
Earth Observation, Field Studies and Modelling
Balzter, H. (Ed.)
2010, XV, 300 p., Hardcover
ISBN: 978-90-481-8640-2